JOURNAL OF MATERIALS SCIENCE 30 (1995) 3799–3804

Phosphor-doped $BaTiO_3$: microstructure development and dielectric properties

A.C. CABALLERO, J.F. FERNÁNDEZ, P. DURÁN, C. MOURE
Electroceramics Department, Instituto de Cerámica y Vidrio, CSIC, 28500 Arganda del Rey, Madrid, Spain

The phosphor cation retards $BaTiO_3$ formation during the first reaction stage, and favours Ba_2TiO_4 formation. As a consequence, the end of the reaction is only accomplished at 1150 °C. The average particle size of the synthesized powder, after attrition milling was < 1.0 μm. Isopressed bars were sintered from 1200–1400 °C. Dilatometric measurements showed the existence of two sintering mechanisms; these were confirmed by means of isothermal sintering experiments. Microstructural development at low sintering temperature differs from that corresponding to higher ones. Very high permittivity values were measured in the 1325–1350 °C sintered samples. This anomalous dielectric behaviour is associated with the presence of phosphor.

1. Introduction

Barium titanate is one of the most important compounds for the fabrication of electroceramic materials, amongst which the multilayer ceramic capacitors have achieved relevant application in recent years. Multilayer devices show a high volumetric capacitive efficiency and hence are widely used in hybrid circuits and integrated microelectronics [1, 2]. Tape-casting is an adequate procedure to prepare multilayer capacitors because of their cheapness and easiness [3]. This procedure requires the preparation of slips which, because of the chemical nature of $BaTiO_3$, must be non-aqueous. The rheological behaviour of slips is adjusted by using several organic additives which play different roles, such as binders, plasticizers, ligands and dispersants [4]. Some of these additives leave residual solids on the ceramic material after heat treatments. Butyl phosphate, which is an excellent dispersant agent, even in very small amounts decomposes leaving P_2O_5 as solid residue. In a previous paper [5], O'Bryan found $Ba_3(PO_4)_2$ crystals on the surface of $BaTiO_3$ ceramic materials and, in his case, the starting anatase was the source of phosphorous impurities. Nevertheless, no paper has been devoted to the study of the effect of P^{5+} cations on the ceramic and electrical behaviour of barium titanate.

Taking into account the extreme sensitivity of this ceramic compound to the presence of impurities, the present work aimed mainly to stablish the influence that the phosphor cation, incorporated as a dopant, may exert on the synthesis and sintering processes of $BaTiO_3$ and on the microstructure development of the ceramic material, because the microstructure is the ceramic parameter which will determine the electrical and mechanical behaviour of the material.

2. Experimental procedure

The raw materials used were TiO_2, (Thann and Mulhose), $BaCO_3$ (Merck CR) and butyl phosphate (Merck CR). These products were characterized as detailed elsewhere [6]. The titanium oxide was chosen because of its very small P_2O_5 content, (< 0.004 wt %). The butyl phosphate was added in a proportion which is equivalent to that conventionally used for preparing $BaTiO_3$ tape-casting slips. The final stoichiometric ratio of the mixture was BaO: $(TiO_2 + P_2O_5) = 1.002$. The amount of P_2O_5 was 0.13 wt % with respect to the $BaTiO_3$.

The mixing procedure was as follows: TiO_2 particles were dispersed in an isopropylic solution of butyl phosphate, by stirring with a high-speed turbine (> 6000 r.p.m.) for 5 min. Then the barium carbonate was added, maintaining the vigorous stirring for a further 10 min. The mixture was oven dried at a temperature near 150 °C. Its thermal evolution was determined by differential thermal analysis (DTA) and thermogravimetric analysis (TGA) techniques. The evolution of the crystalline phases was established by X-ray diffraction (XRD). Data were taken from the peak intensities belonging to each phase present. According to the obtained results, the dried powder was calcined at 1150 °C for 1 h, with the same heating and cooling rate of 3 °C min^{-1}. The calcined powders were attrition milled for 3 h with isopropyl alcohol, dried as above, and sieved through a 63 μm mesh. The particle size was measured using a Sedigraph Technique. The morphology was established using scanning electron microscopy, (SEM). Bars were isopressed at 200 MPa and sintered at temperatures ranging from 1200–1400 °C, with a 2 h constant soaking time, and with heating and cooling rates of 3° C min^{-1}.

0022–2461

The density of the sintered compacts was measured by Archimedes method, with water as the liquid medium. Polished and thermally etched samples were used for microstructural study using SEM and light-reflected optical microscopy (ROM) techniques.

Sliced discs from sintered pellets were electroded by painting with Ag/Pd paste, and subsequent firing at 800 °C for 1/2 h. Dielectric and electric transport parameters were determined as a function of frequency on a vectorial impedance analyser model HP 4192A. The d.c. resistivity was measured using Keithley Model 614 electrometer.

3. Results

Fig. 1 shows the thermogravimetric curves corresponding to the synthesis reaction of $BaTiO_3$ compound. Comparing this curve with that corresponding to phosphor-free mixtures shown elsewhere [6], it was possible to see that the weight losses associated with the carbonate decomposition begin at a temperature somewhat higher when phosphor is present. This is the only difference between both thermal processes. Fig. 2 depicts the evolution of crystalline phase with temperature. One of the most relevant features is the high amount of Ba_2TiO_4 compound which was formed during the intermediate step of the reaction and the displacement of the reaction end towards higher temperatures. At 1150 °C, the reaction seems to be fully completed, and the XRD analysis showed the $BaTiO_3$ as the only phase present. In view of these results the synthesis of barium titanate powders was carried out at that temperature for a soaking time of 2 h.

The attrition milled powder showed an average particle size <1 μm according to the SEM analysis (Fig. 3). Its morphology was rounded, and it formed soft agglomerates with average sizes of about 1.3 μm, as measured by the sedigraph technique.

Fig. 4 shows the curve of densification against temperature for a 2 h constant sintering time. Two different regions can be seen: one from 1225–1275 °C, with slight increases of apparent density up to $<96\%$ D_{th}, and the other from 1300–1400 °C, for which the density remains almost constant over the whole range, with a value of 97.5% D_{th}. Dilatometric experiments, as shown in Fig. 5, show the existence of two different

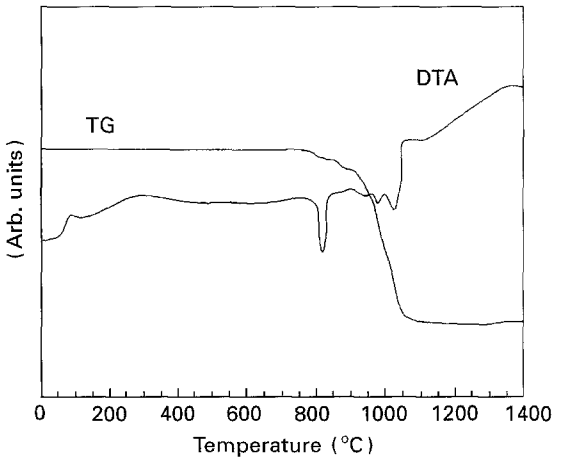

Figure 1 DTA and TG of the mixture $TiO_2 + BaCO_3$ + butyl phosphate.

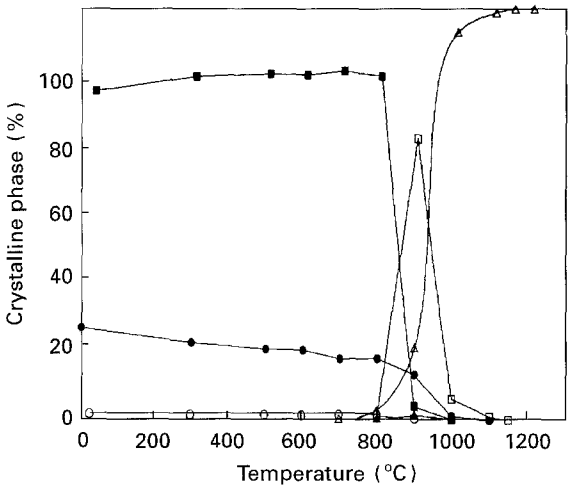

Figure 2 Crystalline phase evolution with temperature of the mixture $TiO_2 + BaCO_3$ + butyl phosphate: (●) TiO_2-rutile, (○) TiO_2-anatase, (■) $BaCo_3$, (□) Ba_2TiO_4, (△) $BaTiO_3$, (▲) other phases.

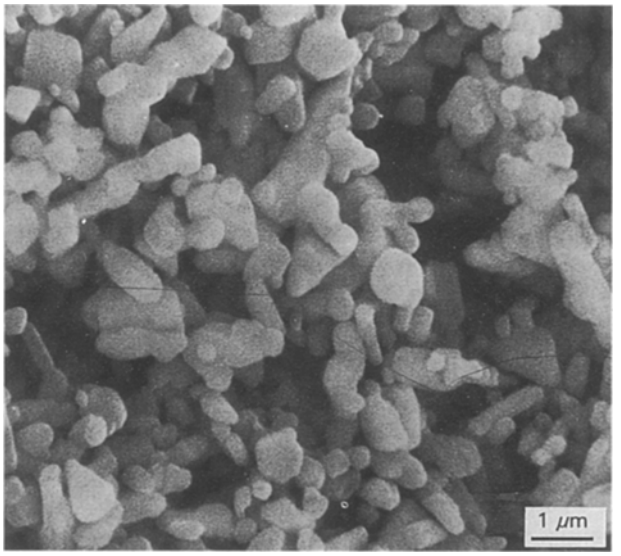

Figure 3 Scanning electron micrograph of synthetized $BaTiO_3$ powder (after attrition milling).

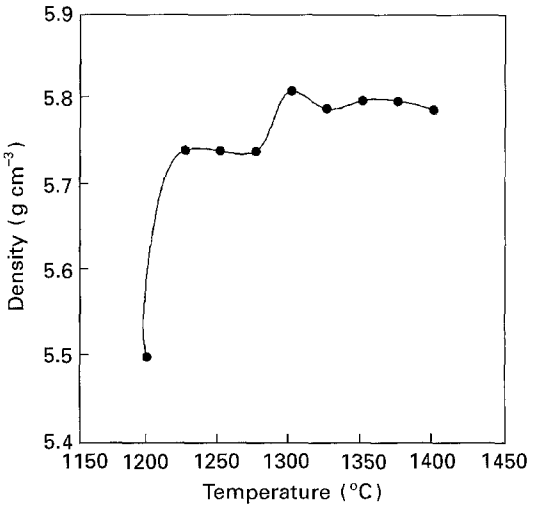

Figure 4 Density versus sintering temperatue (soaking time 2 h).

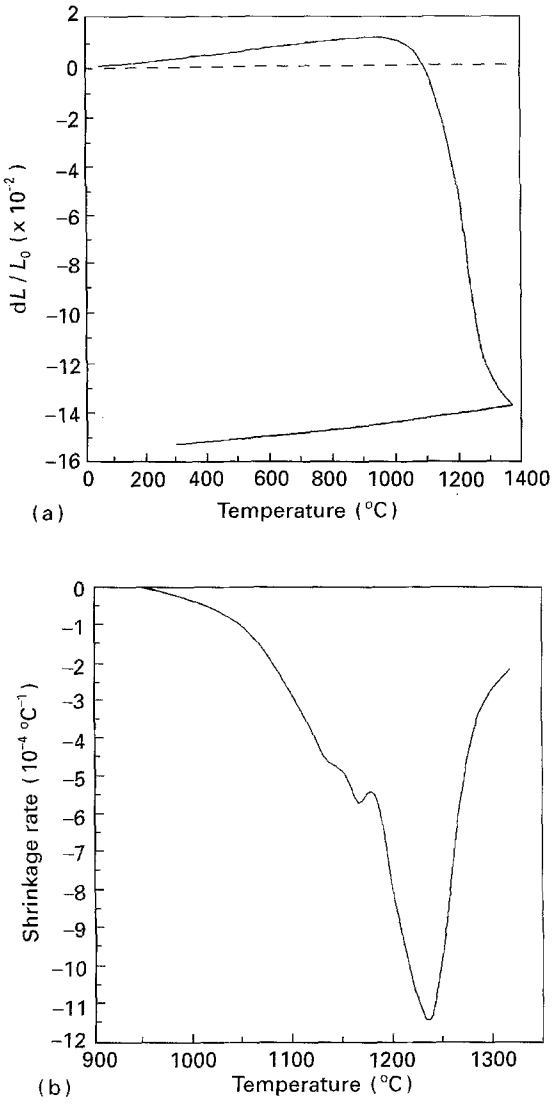

Figure 5 Dilatometric measurements : (a) shrinkage and (b) shrinkage rate, vesus temperature.

shrinkage rate steps. At low temperatures the shrinkage rate was relatively small and grows from higher temperatures. At 1155 °C, which is lower than the temperature of the maximum shrinkage rate, the shrinkage rate diminishes. Such a behaviour is related to the presence of exaggerated grain growth [7].

The microstructural evolution, analyzed by SEM, showed more clearly the difference in the sintering behaviour between the low- and the high-temperature regions. Fig. 6a–c show micrographs corresponding to the samples sintered at 1225, 1250 and 1275 °C, respectively. For 1225 °C there is a bimodal distribution in which very large grains coexist (> 100 μm) together with others with grain sizes < 2 μm, and a considerable porosity, which in some cases, is located inside the larger grains. For a higher sintering temperature up to 1300 °C, the grain growth is more homogeneous, although it is even possible to see pores located in the grain interior. There is no evidence of liquid-phase formation. On the other hand, a crystalline phase located in the triple points and grain boundaries is observed.

For sintering temperatures of 1300 °C and above, a liquid phase can be seen surrounding the grains

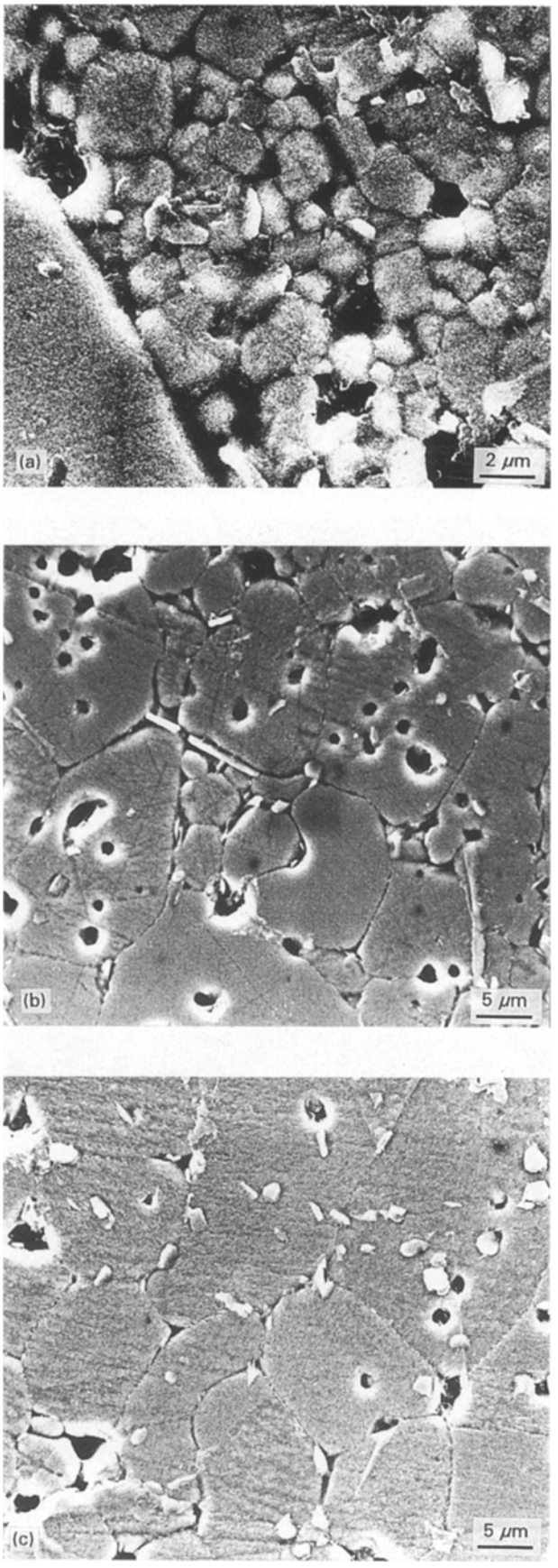

Figure 6 Scanning electron micrographs of polished and thermally etched surfaces of doped samples sintered at (a) 1225 °C, (b) 1250 °C and (c) 1275 °C.

(Fig. 7a–c in samples sintered at 1325, 1350 and 1400 °C, respectively). The average grain size is relatively small and the size distribution is homogeneous for the lowest temperatures of that range. Raising the

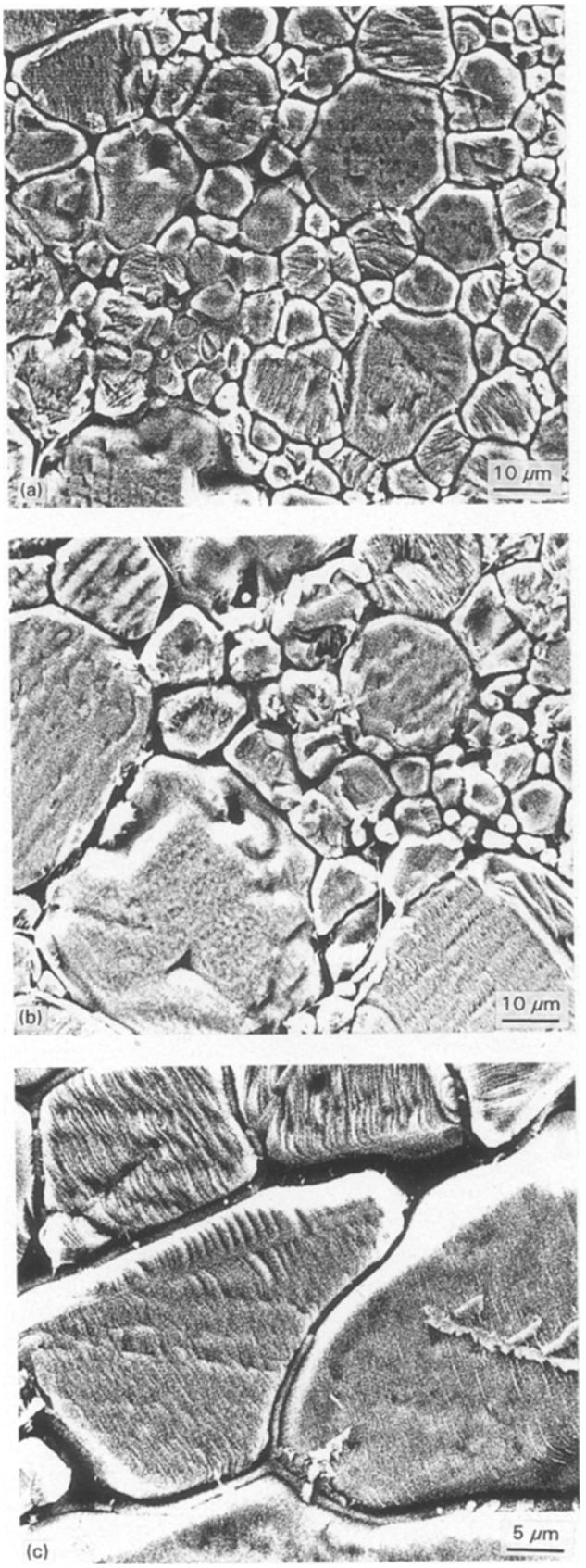

Figure 7 Scanning electron micrographs of polished and thermally etched surfaces of doped samples sintered at (a) 1325 °C, (b) 1350 °C and (c) 1400 °C.

temperature leads to a strong increment of grain size, although there is no porosity in the grain interior. At 1400 °C, the sample is constituted by large grains surrounded by a considerable amount of liquid phase (Fig. 7c).

XRD patterns obtained on the surface of sliced samples sintered at 1275 °C (Fig. 8) allowed the existence of small amounts of a barium phosphate compound, i.e. $Ba_3(PO_4)_2(Ba_3P_2)$, to be establised, which could correspond to the second phase observed by SEM on the low-temperature sintered samples. The peaks vanish for temperatures above 1300 °C. This compound was described previously by McCauley and Hummel [8] and has a melt temperature > 1400 °C.

Table I shows the dielectric constant and loss tangent values for all the sintered samples. For these parameters there is also a significative difference between the samples sintered below and above 1300 °C. The permittivity measurements for samples sintered at low temperatures, such as 1225 °C, gave values which were in agreement with its microstructural development, i.e. < 3000, as measured elsewhere on samples with heterogeneous grain sizes [9] The dielectric losses are relatively high and can be related to the presence of secondary phases located on the grain boundaries. For samples sintered above 1300 °C, extremely high values of permittivity and losses were measured, attaining a maximum for 1325 °C. These values are more normal in the sample sintered at 1400 °C, although the losses remained higher than those corresponding to samples sintered below 1300 °C.

Fig. 9 shows the plot of permittivity versus temperature for doped samples sintered at different temperatures and undoped $BaTiO_3$ sintered at 1275 °C. The

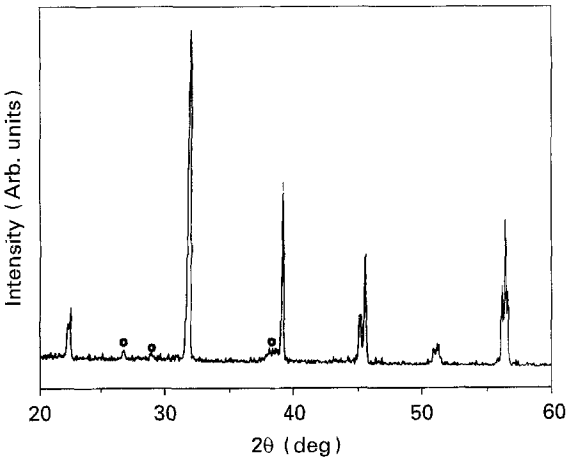

Figure 8 XRD pattern obtained on a polished and thermally etched surface of the sample sintered at 1275 °C.

TABLE I Dielectric constant and dielectric losses measured at $f = 1$ kHz for doped samples sintered at different temperatures

Sintering temperature (°C)	ε	Tan δ (%)
1200	2245	5.6
1225	2649	4.6
1250	3603	9.4
1275	3244	8.6
1300	6000–8000	18–23
1325	11000–14000	19–23
1350	9000–12000	17–20
1375	4200	9.2
1400	5790	11

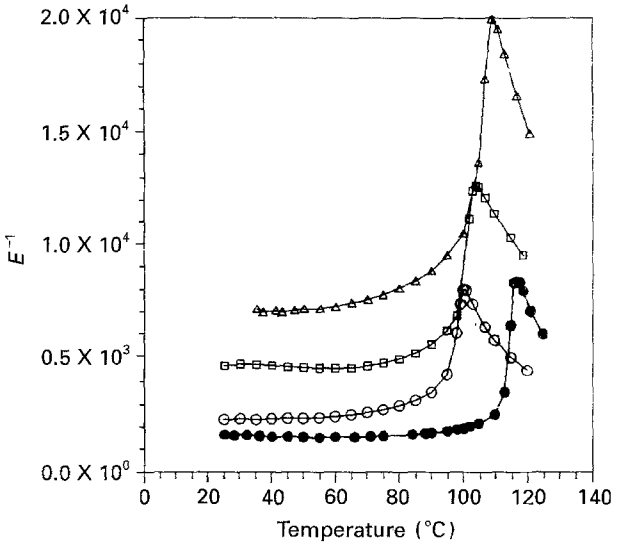

Figure 9 Permittivity versus temperature for (○, □, △) doped samples sintered at different temperatures and (●) undoped $BaTiO_3$ sintered at 1275 °C: (○) 1250 °C, (□) 1300 °C, (△) 1400 °C.

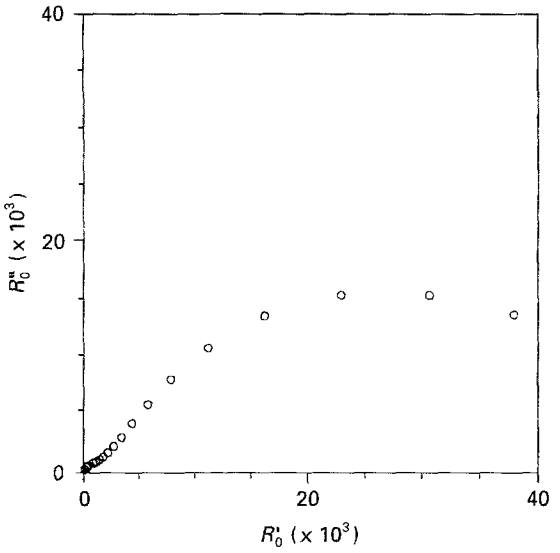

Figure 11 Impedance diagram of the sample sintered at 1400 °C, obtained at 425 °C.

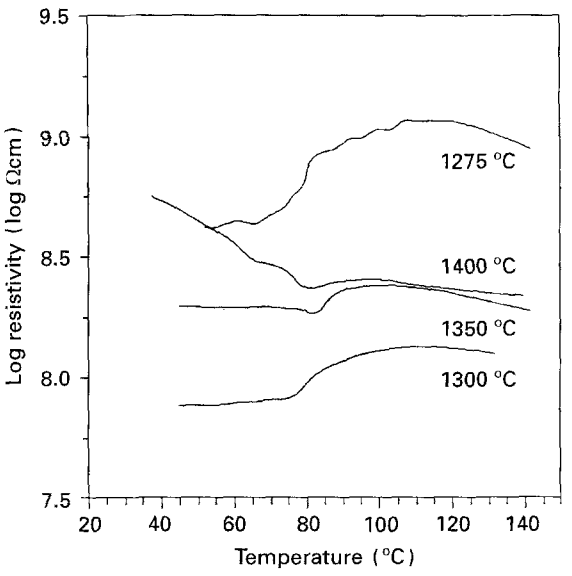

Figure 10 Resistivity versus temperature for doped samples sintered at different temperatures, showing the PTCR effect.

Curie temperature is lower for doped samples, indicating a mechanism of incorporating P^{5+} into the $BaTiO_3$ lattice. On the other hand, when the sintering temperature is higher and the amount of second phase increases, the Curie temperature of the doped samples is closer to the value observed for undoped $BaTiO_3$.

D.C. resistivity measurements against temperature (Fig. 10) showed a relatively small positive temperature coefficient of resistance (PTCR) effect which is more pronounced for the samples sintered between 1300 and 1350 °C. In addition, the room-temperature resistivity is lower for these samples than for the remainder. On the other hand, the experiments performed by complex impedance spectroscopy at several temperatures proved that the grain interior has higher conductivity values than those corresponding to the grain boundaries (Fig. 11). Table II gives the values of bulk and grain-boundary conductivities for samples sintered at several temperatures.

TABLE II A.c conductivity of grain (σ_b) and grain boundary (σ_{gb}) measured at 425 °C of doped samples sintered at different temperatures

Sintering temperature (°C)	A.c. conductivity ($\Omega\ cm^{-1}$) σ_b	σ_{gb}
1250	7.24×10^{-5}	9.66×10^{-6}
1300	1.41×10^{-4}	8.31×10^{-6}
1350	3.10×10^{-4}	2.12×10^{-6}
1400	3.40×10^{-4}	2.02×10^{-5}

4. Discussion

From the data corresponding to the synthesis process it is possible to assume that the phosphor cation plays a retarding role on the reaction kinetics between $BaCO_3$ and TiO_2. The reason for this behaviour may be related to the location of the P^{5+} cations on the TiO_2 particle surfaces. It has been well established that the titanium dioxide produces a strong increase in the $BaCO_3$ decomposition kinetics. The presence of the P^{5+} cation could cause a decrease in those kinetics and therefore a displacement of the onset of the decomposition towards higher temperatures. However, because of the higher temperature, when $BaCO_3$ decomposition begins, it takes place at a higher decomposition rate, leading to the presence of a greater amount of barium cations per unit time in the vicinity of the TiO_2 particle surfaces. As a consequence, the formation of Ba_2TiO_4 will be favoured. According to the model proposed by Beauger *et al.* [10], the formation of orthotitanate retards the end of the reaction, in order to reach higher temperatures for the accomplishment of $BaTiO_3$ synthesis. Despite this increment in the synthesis temperature, the final particle size was held within relatively small values, probably owing to the high dispersion grade of the reactant powders caused by the surface location of phosphor cations.

The sintering behaviour seems to be strongly affected by the presence of phosphor. The surface location of P^{5+} allowed the formation of Ba_3P_2 during the

initial sintering step. A simple numerical calculation indicates that this formation of Ba_3P_2 displaces the Ba/Ti ratio towards a value < 1.00. This displacement favours the appearance of an exaggerated grain growth mechanism [11], whereas liquid-phase formation is inhibited because of the high melting point of the barium phosphate. When the sintering temperature is raised, the tendency of P^{5+} to be incorporated into the $BaTiO_3$ lattice increases and, therefore, the Ba/Ti ratio for the grain bulk raised, leading to a gradual disappearance of the exaggerated grain-growth process. On the other hand, the Ti^{4+} cations are displaced from bulk to grain boundary due to the phosphor incorporation. These titanium cations can form a liquid phase belonging to the ternary system $BaO–TiO_2–P_2O_5$.

The presence of crystalline phase Ba_3P_2 during the first sintering step, by acting as a barrier to volume diffusion which is the controlling mechanism of the initial sintering step, could be the reason for the observed slow shrinkage rate. Its location on the grain boundaries, as seen in scanning electron micrographs agrees well with such an assumption. The appearance of a liquid phase when the temperature rises can act as a lubricant medium for the accommodation of grains, leading to the increment in the shrinkage rate observed on the dilatometric curves.

The very high value of the measured permittivity on samples sintered at temperatures for which P^{5+} could be located in the Ti^{4+} lattice sites via solid solution formation, must be correlated with the appearance of a bulk semiconducting behaviour caused by the presence of Ti^{3+} which is promoted to compensate for the excess valence of the nearest neighbour P^{5+}. This mechanism is the same as that described for Nb^{5+} substitution [12]. Because of the low values of the grain-boundary conductivity, the dielectric behaviour of the samples sintered at 1325–1350 °C could be assimilated to the grain-boundary barrier layer model (GBBL), the corresponding measured permittivity values to an "effective dielectric constant" for the bulk sample, and not to the polarizability of the ceramic grains.

The observed weak PTCR phenomenon correlates well with all the above described mechanism of phosphor incorporation. The decrease of the permittivity values for samples sintered above 1350 °C could be attributed to a new segregation process which takes place with exsolution of phosphor cations towards grain boundaries, and simultaneous titanium vacancy formation that produces an increase in the bulk resitivity and the subsequent attenuation in the PTCR phenomenon. The microstructure of the samples sintered at 1400 °C, as shown in Fig. 7, seems to confirm this hypothesis.

5. Conclusions

The presence of P^{5+} as an impurity in the raw materials for barium titanate produces an increase in the temperature of the maximum synthesis reaction because of the formation of orthotitanate as an intermediate phase. P^{5+} is a very common impurity in anatase.

During sintering at low temperatures, P^{5+} induces an exaggerated grain growth mechanism, which disappears when the sintering temperature is raised. Above 1300 °C, phosphor doping promotes liquid-phase formation, which may be very abundant despite the small amount of P_2O_5 present.

At intermediate temperatures, P^{5+} may enter the $BaTiO_3$ lattice, substituting for Ti^{4+} and causing an increase in the bulk conductivity.

The deleterous effect of the presence of P^{5+} must be taken into account with regard to the dispersant agent election when slips for tape-casting are prepared.

References

1. I. BURN, M. T. RAAD and K. SASAKI, in "Ceramic transactions", Vol. 8, edited by H. C. Ling and M. F. Yan (American Ceramic Society Inc., Westerville, OH, 1990) pp. 20–34.
2. Y. SAKABE, T. TAKAGI, K. WAKINO and D. M. SMYTH, "Advances in ceramics", Vol. 19, edited by J. B. Blum and W. R. Cannon (American Ceramic Society Inc., Westerville, OH, 1986) pp. 103–15
3. K. R. MIKESKA and W. R. CANNON *Coll. Surf.* **29** (1988) 305.
4. W. R. CANNON, J. R. MORRIS and K. R. MIKESKA, in "Advances in ceramics", Vol. 19, edited by J.B. Blum, and W. R. Cannon (American Ceramic Society Inc., Westerville, OH, 1986) pp. 161–74
5. H. M. O'BRYAN Jr, *Am. Ceram. Soc. Bull.* **66** (1987) 677.
6. J. F. FERNÁNDEZ, P. DURÁN and C. MOURE, *J. Mater. Sci.* **26** (1991) 3257.
7. A. C. CABALLERO, PhD thesis, Universidad Autónoma de Madrid, Madrid (1994).
8. R. A. McCAULEY and F. A. HUMMEL, *Trans. Brit. Ceram. Soc.* **67** (1968) 619.
9. J. S. CHOI and H. G. KIM, *J. Mater. Sci.* **27** (1992) 1285.
10. A. BEAUGER, J. C. MUTIN and J. C. NIEPCE, *J. Mater. Sci.* **18** (1983) 2543.
11. A. K. MAURICE and R. C. BUCHANAN, *Ferroelectrics*, **74** (1987) 61.
12. J. F. FERNÁNDEZ, P. DURÁN and C. MOURE *ibid.* **106** (1990) 381.

Received 3 November 1994
and accepted 20 January 1995